Electronic Supplementary Material (ESI) for Materials Chemistry Frontiers.

Hollow viologen-based porous organic polymer for catalytic cycloaddition of CO_2

Hao Luo, Shun Wang, Xianyu Meng, Gang Yuan, Xiaowei Song* and Zhiqiang Liang*

State Key Lab of Inorganic Synthesis and Preparative Chemistry, College of Chemistry, Jilin University, Changchun, 130012, P. R. China.

E-mail: xiaoweisong@jlu.edu.cn (X. Song); liangzq@jlu.edu.cn (Z. Liang).

Synthesis of viologen monomer

As shown in Scheme S1, 1,1’-bis(2,4-dinitrophenyl)-[4,4’-bipyridine]-1,1’-diium dichloride and 1,1’-bis(4-bromophenyl)-4,4’-bipyridinium chloride (Monomer-1) were prepared with high yield.

Synthesis of Zincke Salt. 4,4-Bipyridine (1.92 g, 12 mmol) and 1-Chloro-2,4-dinitrobenzene (7.11 g, 35 mmol) were dispersed in 40 mL acetonitrile in a 100 mL round bottom flask. Degassed immediately by three freeze-pump-thaw cycles and keep the reaction reflux for 72 h. The solid product obtained by filtration after the system cooled to room temperature, and washed by sufficient acetone. After drying in vacuum at 80 °C for 12 h, the brown yellow solid powder was collected.

Synthesis of Monomer 1. The successful preparation of 1,1’-bis(4-bromophenyl)-4,4’-bipyridinium chloride (Monomer-1) was with reference to the reported work[1].

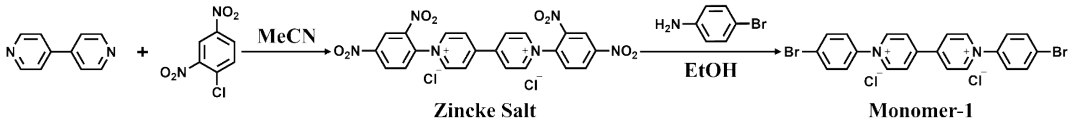

Scheme S1. Synthetic route of Monomer-1.

Synthesis of nano silica spheres. A 250 mL round-bottomed flask was charged with ethanol (74 mL), water (10 mL) and ammonia water (3.15 mL). After forming a homogeneous mixture at room temperature, 6 mL of tetraethyl orthosilicate (TEOS) was added. After stirring for one hour at room temperature, the nano SiO_2 spheres were collected by centrifugation, washed with water and ethanol. After drying in a vacuum oven at 80 °C for 12 h, the nano SiO_2 spheres with uniform size (ca. 240 nm) were obtained as a white solid powder.

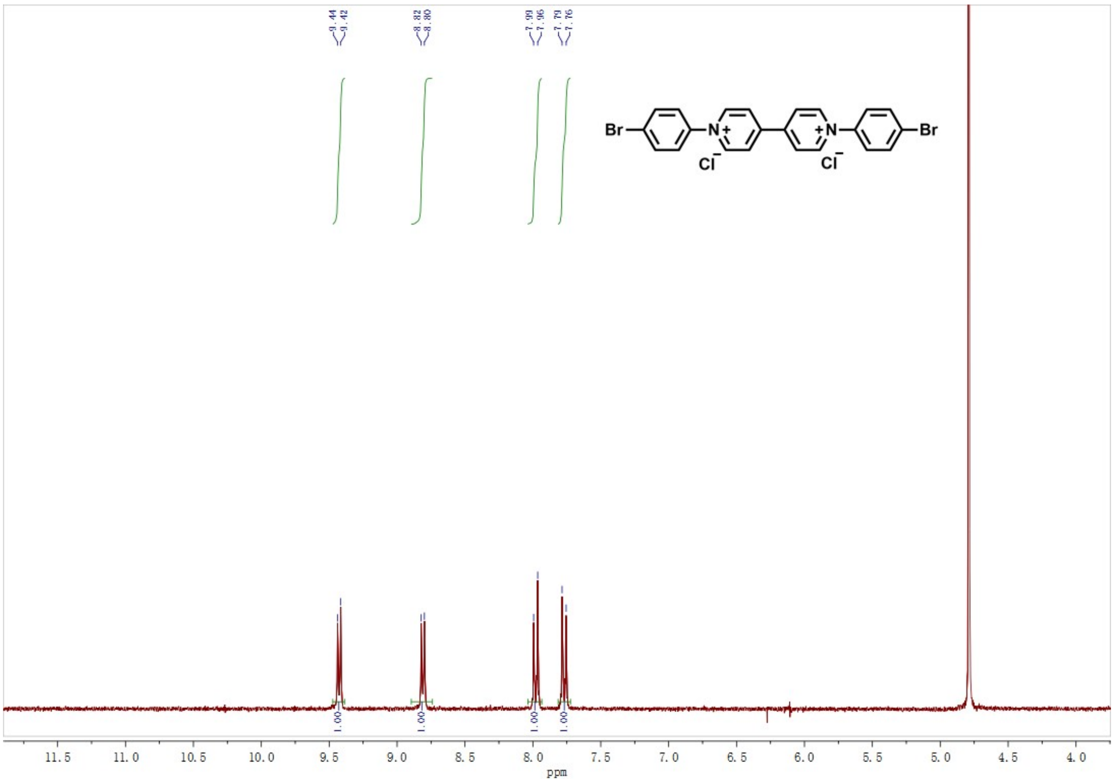

Fig. S1 ^{1}H NMR spectra of Monomer-1 in D_2O.

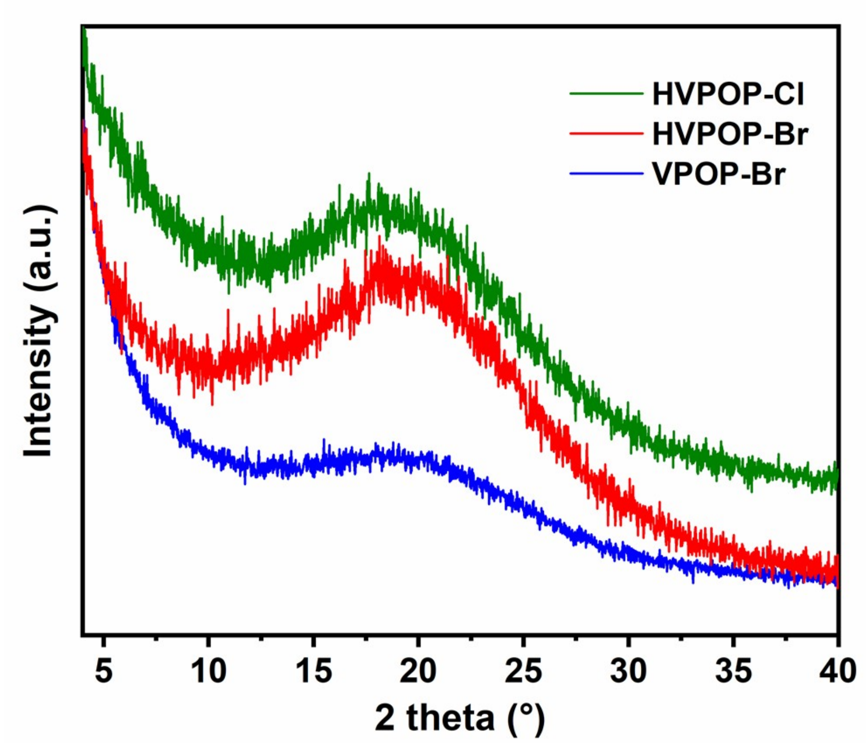

Fig. S2 PXRD curves of (H)VPOPs.

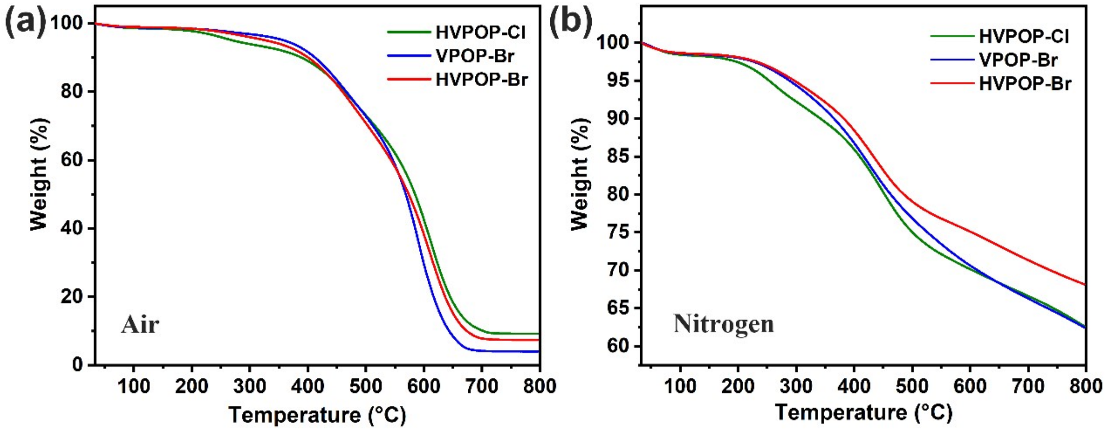

Fig. S3 Thermogravimetric analysis (TGA) of (H)VPOPs under air (a) and N_2 (b) atmosphere in the range from 30 °C to 800 °C.

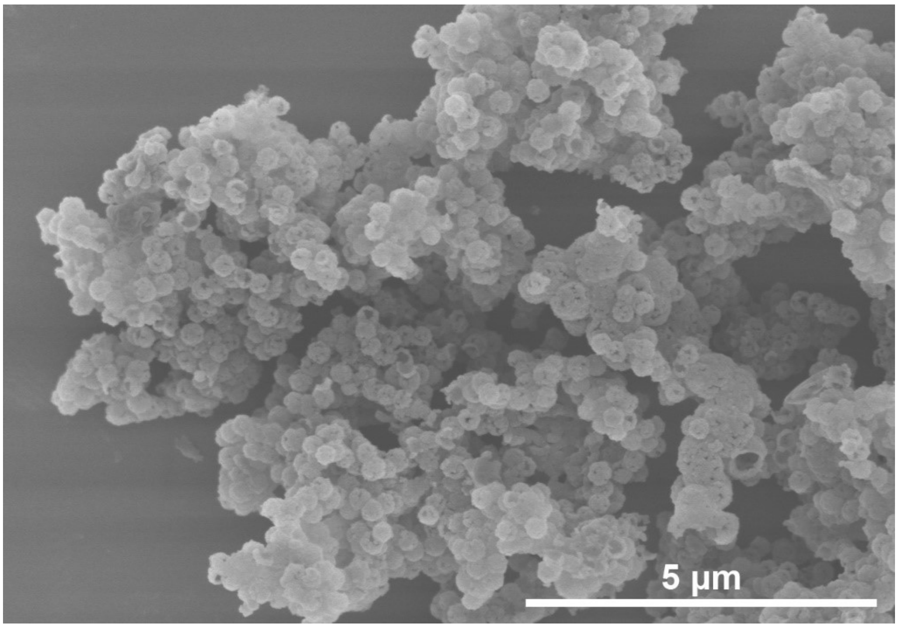

Fig. S4 SEM image of HVPOPs.

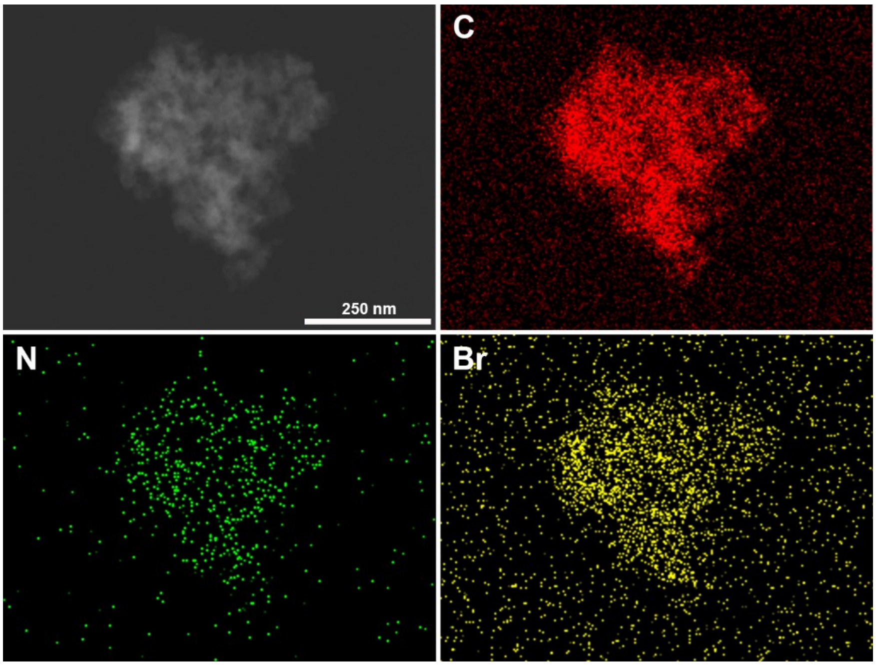

Fig. S5 TEM and Energy-dispersive X-ray spectrometry (EDS) elemental mapping images including C, N, Br elements for the sample VPOP-Br.

Calculations of the Isosteric Heats of Gas Adsorption (Q_{st})^2

The isosteric heat was calculated by the Virial equation:

$$lnP = lnN + \frac{1}{T}\sum_{i=0}^{m} aiN^i + \sum_{i=0}^{n} biN^i$$

$$Q_{st} = -R\sum_{i=0}^{m} aiN^i$$

P: the pressure;

N: the adsorbed amount;

T: the temperature;

ai and ***bi***: virial coefficients;

m and ***n***: the number of coefficients used to describe the isotherms;

R: gas constant (8.314 kJ mol^{-1})

Q_{st}: isosteric heat which reflect the interactions between the gas molecule and the materials.

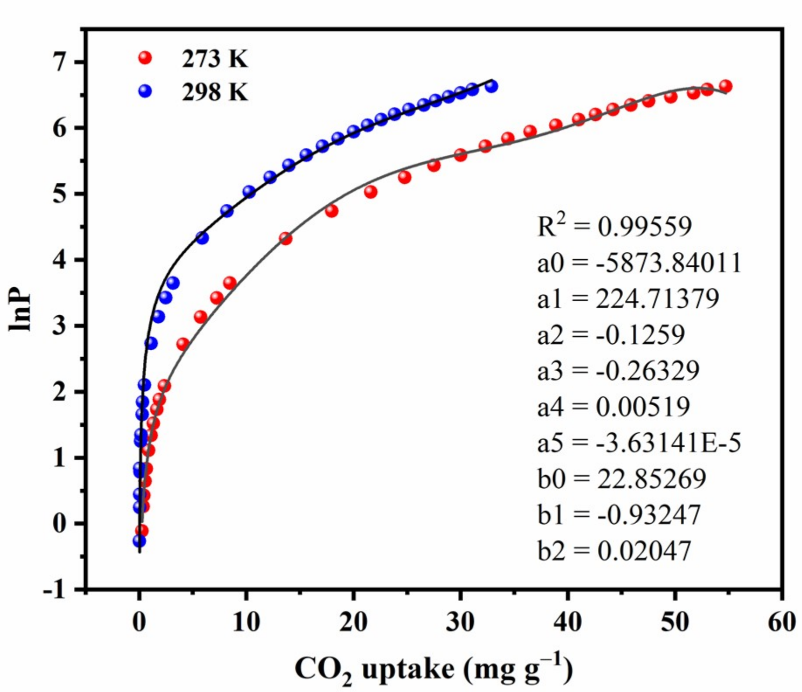

Fig. S6 Virial fitting for CO_2 isotherms of HVPOP-Cl.

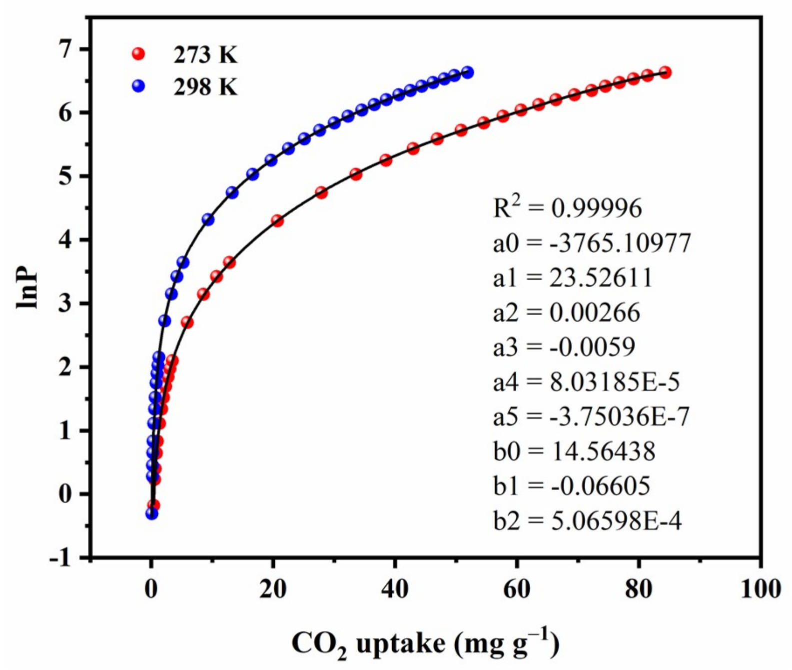

Fig. S7 Virial fitting for CO_2 isotherms of VPOP-Br.

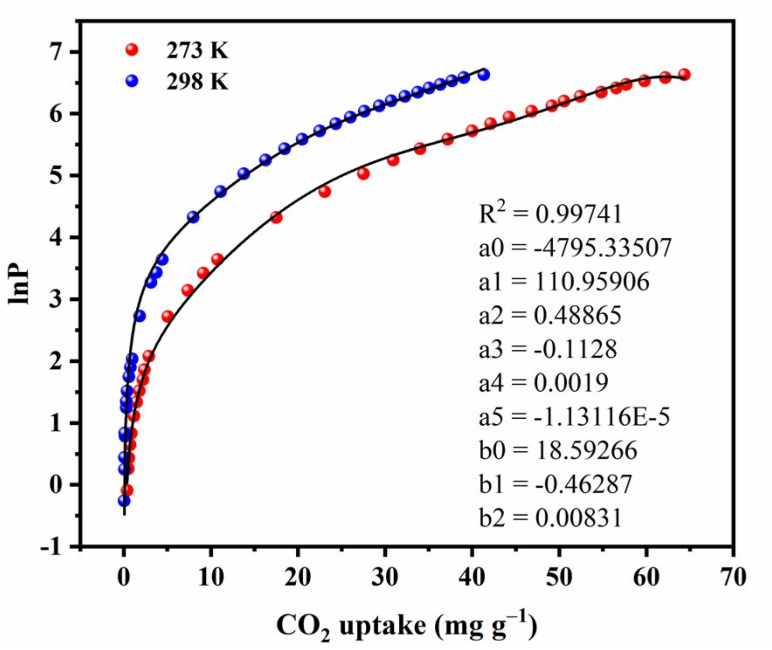

Fig. S8 Virial fitting for CO_2 isotherms of HVPOP-Br.

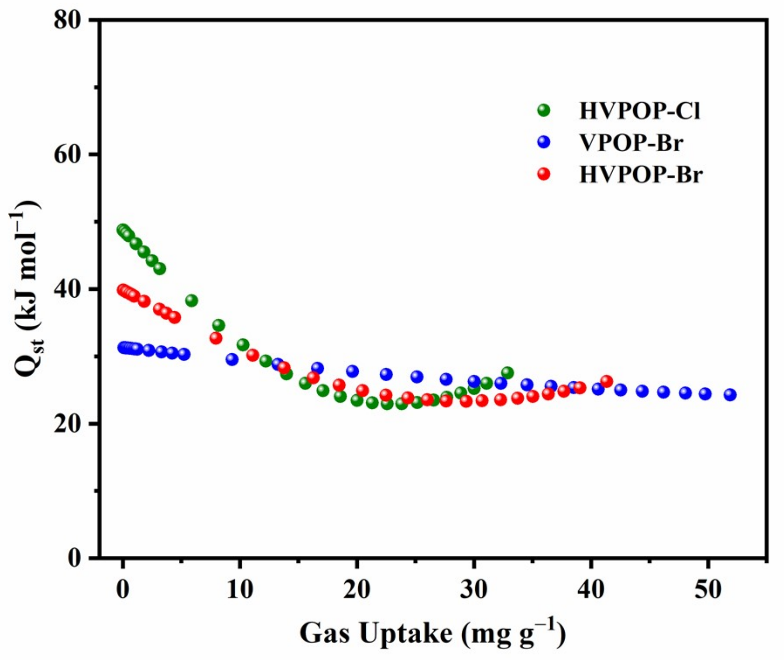

Fig. S9 Adsorption enthalpy of (H)VPOPs for CO_2.

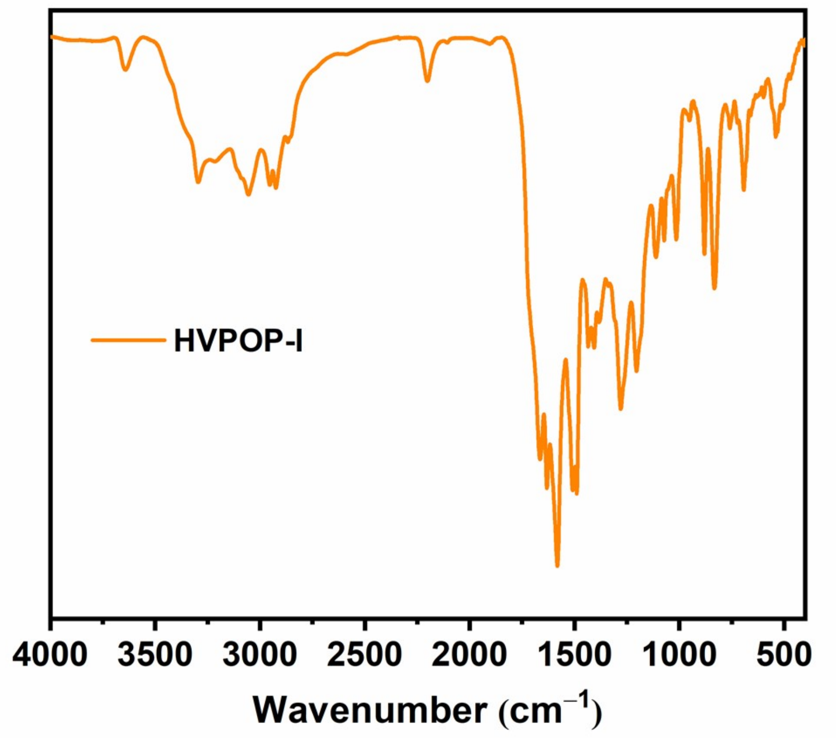

Fig. S10 FT-IR spectra of HVPOP-I.

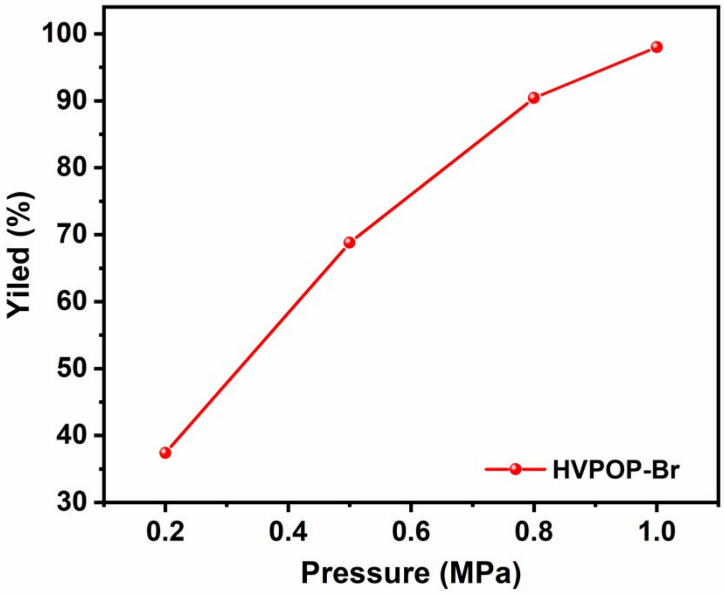

Fig. S11 The kinetic curve of cycloaddition reaction of epichlorohydrin depending on CO_2 pressure at 120 °C and with 60 mg HVPOP-Br for 12 h.

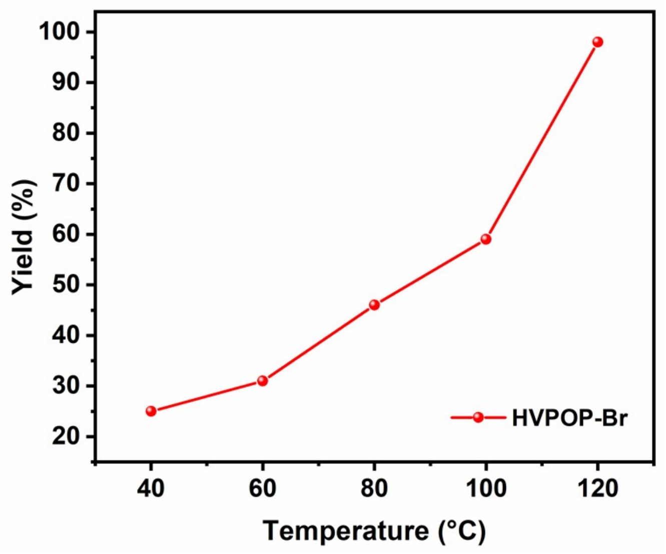

Fig. S12 The kinetic curve of cycloaddition reaction of epichlorohydrin depending on reaction temperature under 1 MPa CO_2 and with 60 mg HVPOP-Br for 12 h.

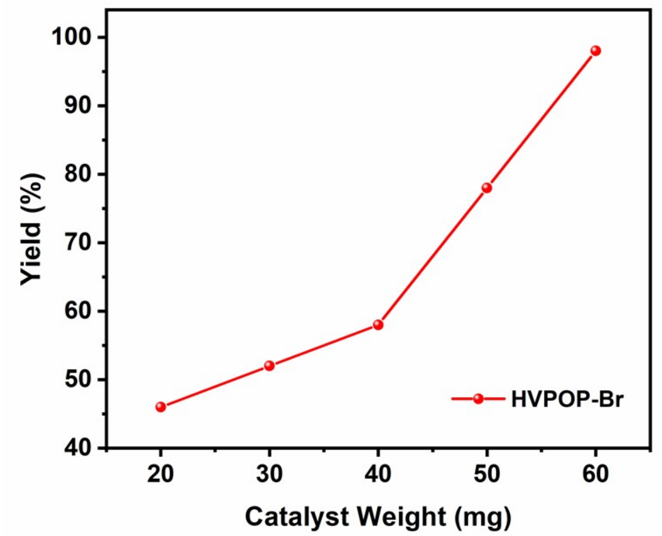

Fig. S13 The kinetic curve of cycloaddition reaction of epichlorohydrin depending on catalyst weight under 1 MPa CO_2 at 120 °C for 12 h.

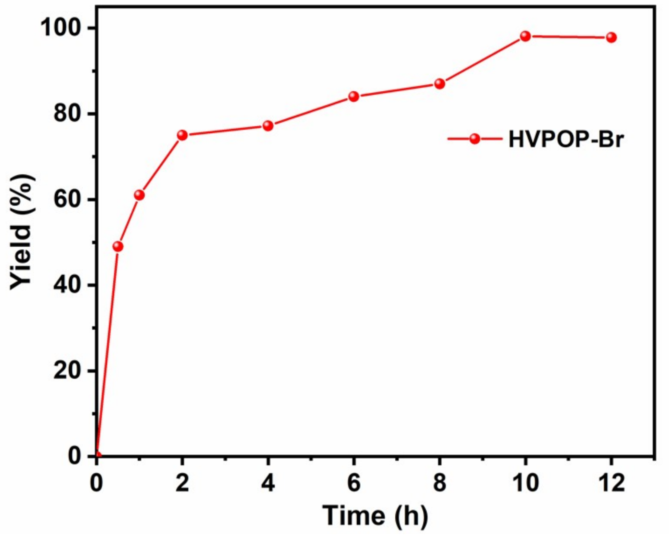

Fig. S14 The kinetic curve of cycloaddition reaction of epichlorohydrin depending on reaction time under 1 MPa CO_2 with 60 mg HVPOP-Br at 120 °C.

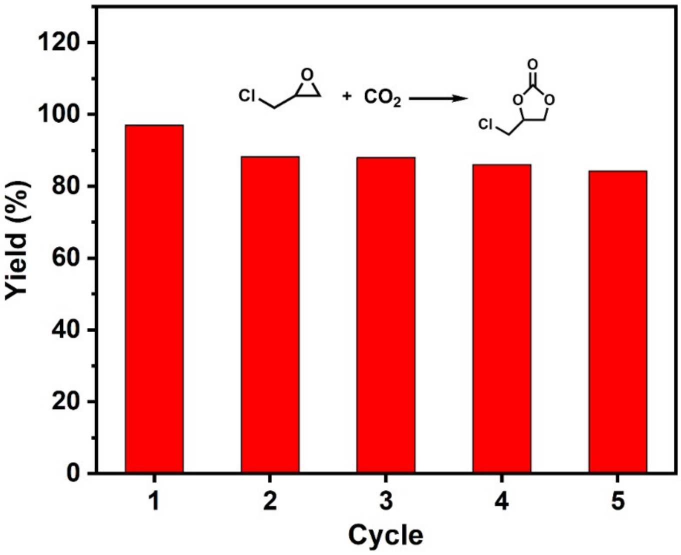

Fig. S15 Catalytic reusability of HVPOP-Br in the cycloaddition of CO_2 with epichlorohydrin. Reaction conditions: epichlorohydrin (10 mmol), HVPOP-Br (60 mg), CO_2 pressure (1 MPa), 120 °C, 12 h.

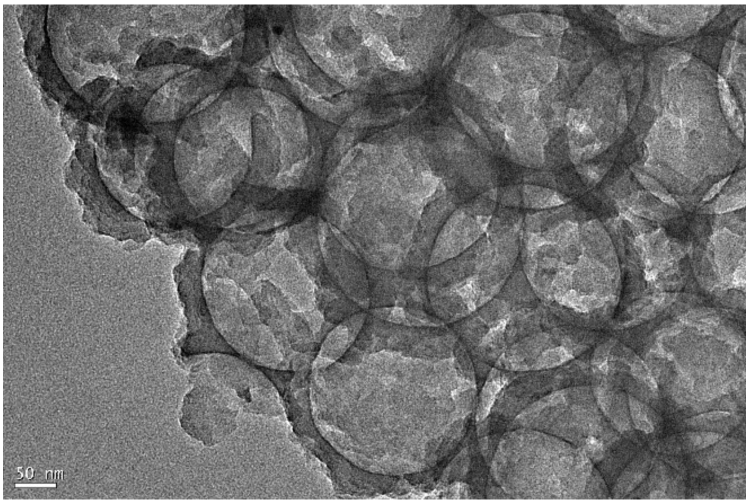

Fig. S16 TEM image of HVPOP-Br after cycloaddition reaction.

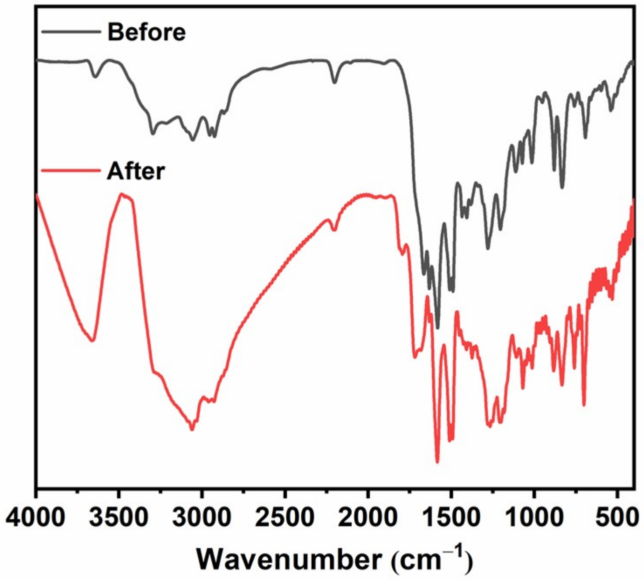

Fig. S17 FT-IR spectra of HVPOP-I after cycloaddition reaction.

The process of yield calculation by ^{1}H NMR[3]

After the reaction is completed, part of crude products of various substrates are directly taken out, dissolved in a deuterated reagent, filtered and tested by Varian Mercury spectrometer operating at frequency of 300 MHz. The yields of various substrates to their own cyclic carbonates catalyzing by HVPOP-Br were calculated according to the following equation.

$$Yield(\%) = \frac{I_{H_{a'}}}{I_{H_a} + I_{H_{a'}}} \times 100\%$$

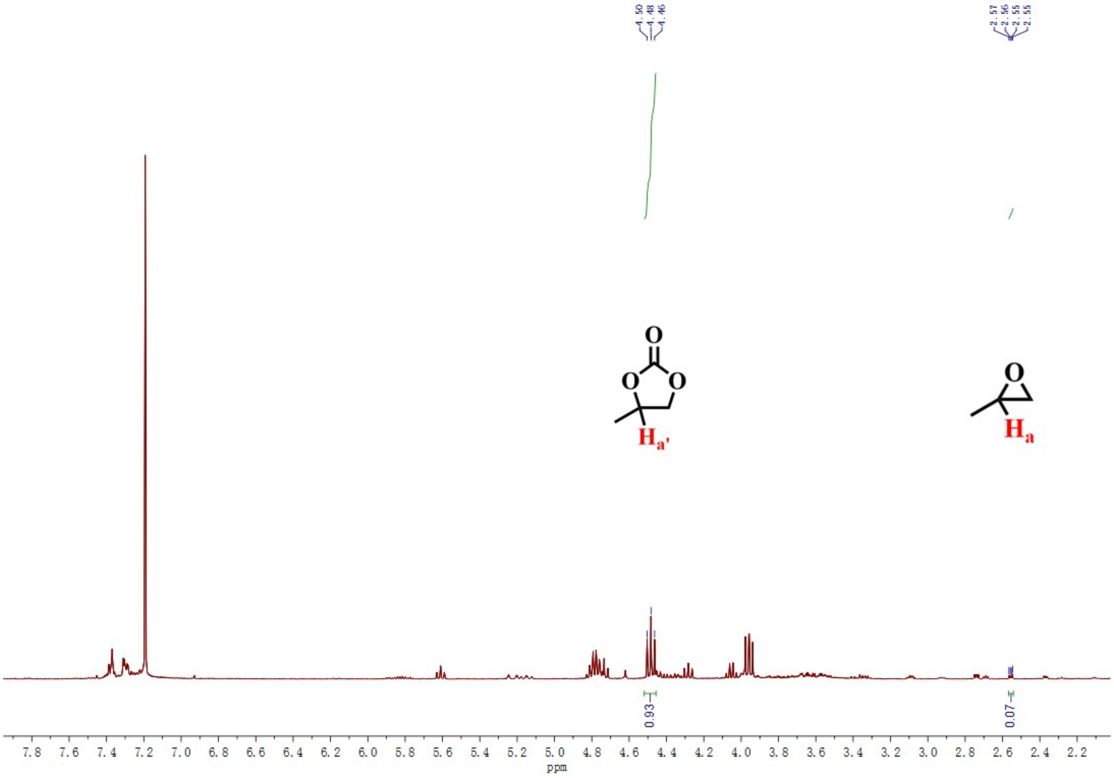

Fig. S18 ^{1}H NMR spectrum of the propylene oxide's crude product after catalyzed by HVPOP-Br in $CDCl_3$.

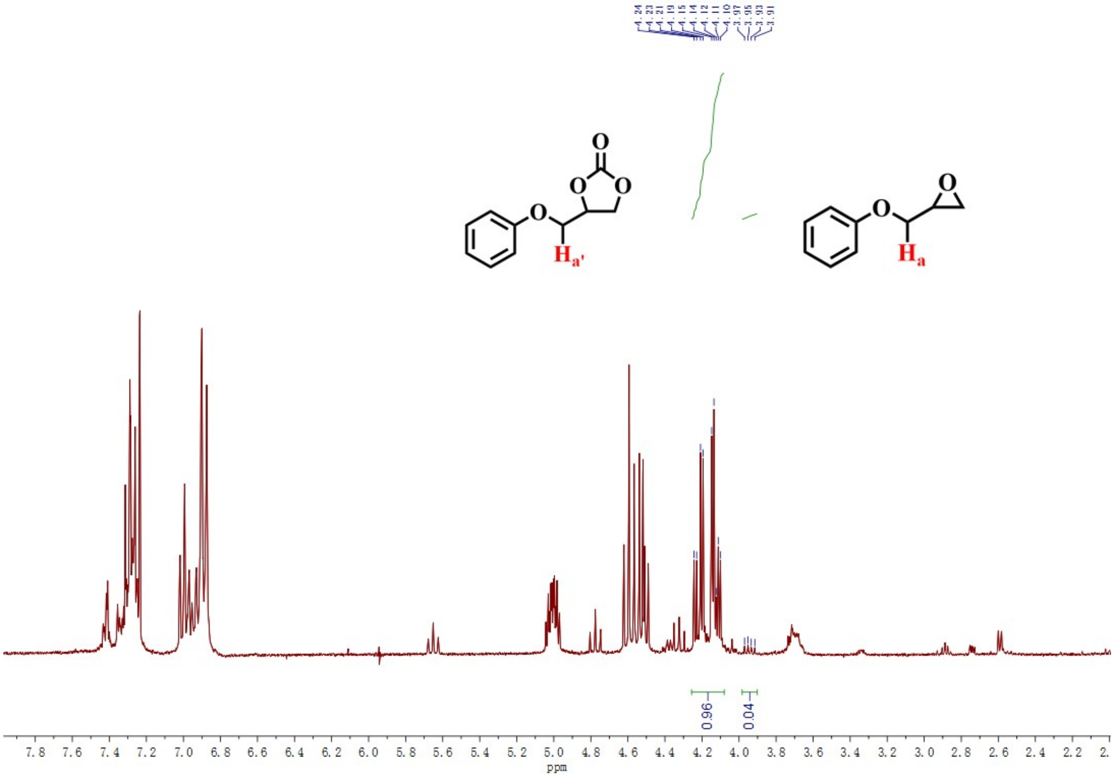

Fig. S19 ^{1}H NMR spectrum of the phenyl glycidyl ether's crude product after catalyzed by HVPOP-Br in $CDCl_3$.

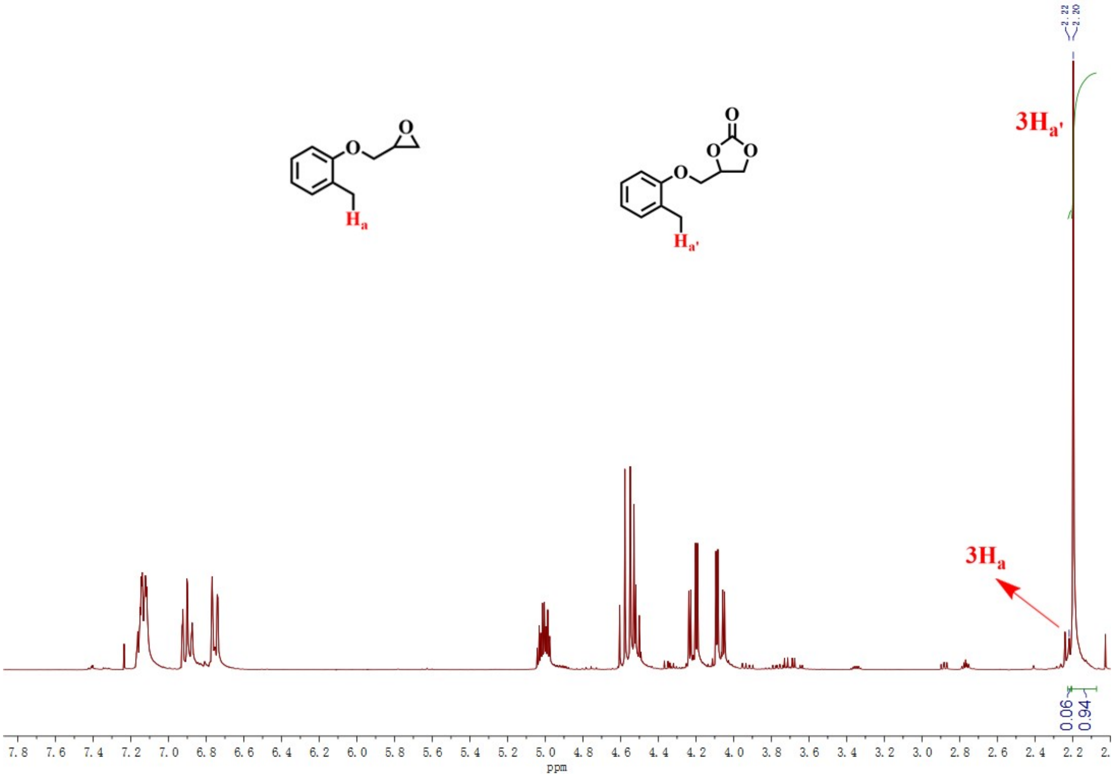

Fig. S20 ^{1}H NMR spectrum of the o-tolyl glycidyl ether's crude product after catalyzed by HVPOP-Br in $CDCl_3$.

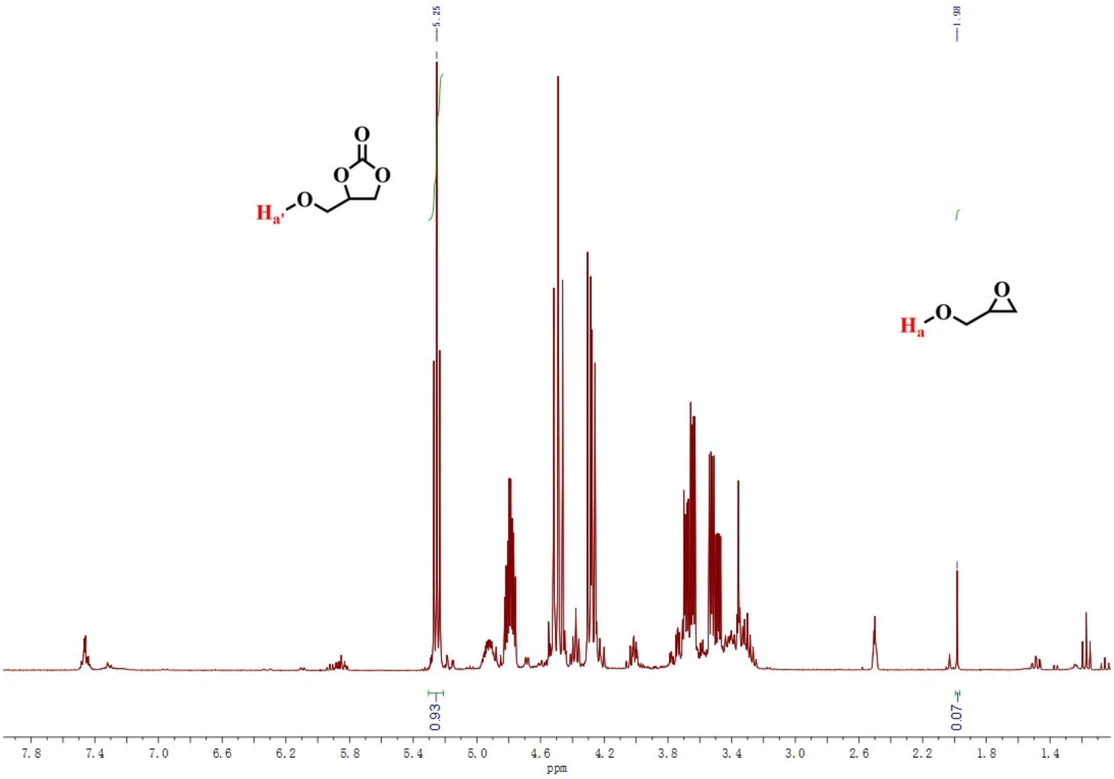

Fig. S21 ^{1}H NMR spectrum of the glycidol's crude product after catalyzed by HVPOP-Br in DMSO-d_6.

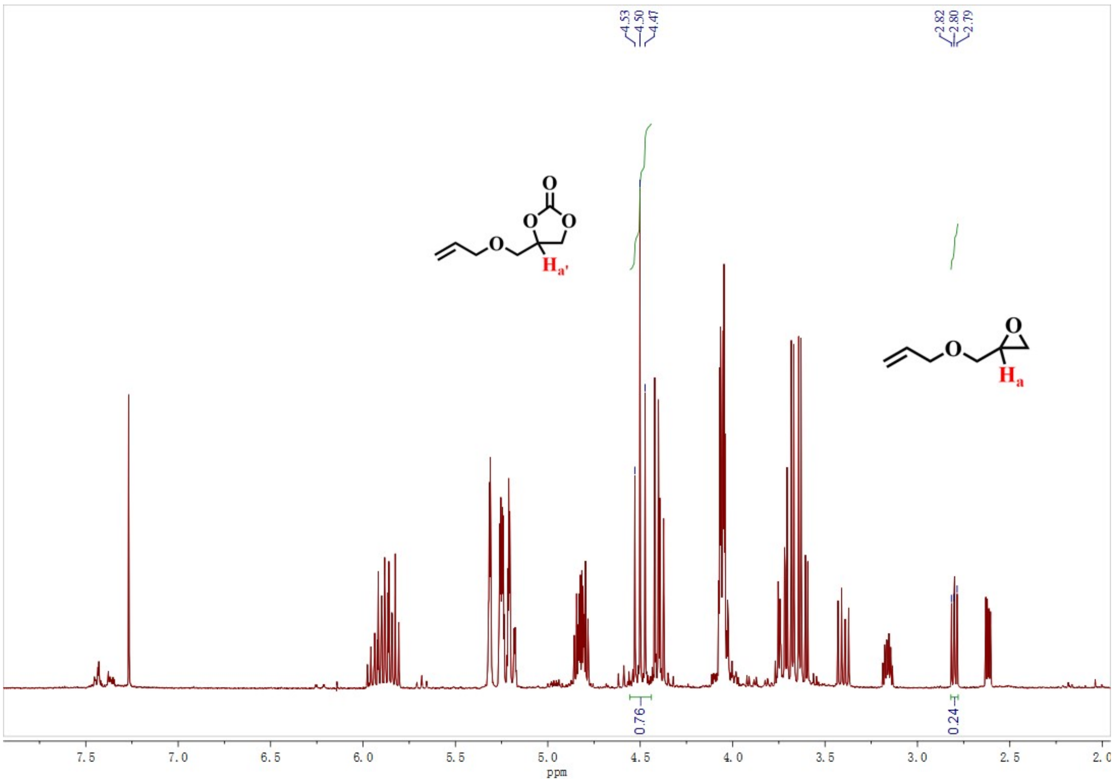

Fig. S22 ^{1}H NMR spectrum of the allyl glycerol ether's crude product after catalyzed by HVPOP-Br in $CDCl_3$.

Table S1. Comparison with different viologen-based catalysts reported in the reaction of CO_2 with Styrene oxide[4-8].

Catalyst	m(Cat.) (mg)	Epoxide	Pressure (MPa)	T (°C)	t (h)	Yield (%)	Ref.
HVPOP-Br	60	10 mmol	1	120	12	85	**This work**
VIP-Br	50	2 mmol	0.1	80	48	98	S4
V-iPHP-1	50	2 mmol	0.1	80	72	93	S5
V-PCIF-Br	50	5 mmol	1	100	6	98	S6
Zn-ICOP	0.16 mol%	1 mL	1	80	12	4	S7
cCTF-500	CO_2/cCTF-500 (4 wt%)		1	90	12	36	S8

Reference

1. C. Hua, B. Chan, A. Rawal, F. Tuna, D. Collison, J. M. Hook and D. M. D'Alessandro, Redox tunable viologen-based porous organic polymers, *J. Mater. Chem. C*, 2016, **4**, 2535−2544.
2. X. Y. Meng, Y. C. Liu, S. Wang, J. F. Du, Y. Ye, X. W. Song and Z. Q. Liang, Silsesquioxane–Carbazole-Corbelled Hybrid Porous Polymers with flexible nanopores for efficient CO_2 conversion and luminescence sensing, *ACS Appl. Polym. Mater.*, 2019, **2**, 189−197.
3. G. Yuan, Y. Lei, X. Y. Meng, B. D. Ge, Y. Ye, X. W. Song and Z. Q. Liang, Metal-assisted synthesis of salen-based porous organic polymer for highly efficient fixation of CO2 into cyclic carbonates, *Inorg. Chem. Front.*, 2022, **9**, 1208−1216.
4. Y. D. Zhang, K. Zhang, L. Wu, K. Liu, R. Huang, Z. Y. Long, M. M. Tong and G. J. Chen, Facile synthesis of crystalline viologen-based porous ionic polymers with hydrogen-bonded water for efficient catalytic CO_2 fixation under ambient conditions, *RSC Adv.*, 2020, **10**, 3606−3614.
5. Y. D. Zhang, K. Liu, L. Wu, H. Zhong, N. Luo, Y. X. Zhu, M. M. Tong, Z. Y. Long and G. J. Chen, Silanol-Enriched Viologen-Based Ionic Porous Hybrid Polymers for efficient catalytic CO_2 fixation into cyclic carbonates under mild conditions, *ACS Sustain. Chem. Eng.*, 2019, **7**, 16907−16916.
6. G. J. Chen, X. H. Huang, Y. D. Zhang, M. Y. Sun, J. Shen, R. Huang, M. M. Tong, Z. Y. Long and X. C. Wang, Constructing POSS and viologen-linked porous cationic frameworks induced by the Zincke reaction for efficient CO_2 capture and conversion, *Chem. Commun.*, 2018, **54**, 12174−12177.
7. S. T. Kostakoğlu, Y. Chumakov, Y. Zorlu, A. E. Sadak, S. Denizaltı, A. G. Gürek and M. M. Ayhan, Elucidating the role of non-covalent interactions in unexpectedly high and selective CO_2 uptake and catalytic conversion of porphyrin-based ionic organic polymers, *Mater. Adv.*, 2021, **2**, 3685−3694.
8. O. Buyukcakir, S. H. Je, S. N. Talapaneni, D. Kim and A. Coskun, Charged Covalent Triazine Frameworks for CO_2 capture and conversion, *ACS Appl.*

Mater. Interfaces, 2017, **9**, 7209−7216.